DMD Fast Forward. Published on September 19, 2007 as doi:10.1124/dmd.107.017384

DMD #17384

Cyclic conversion of the Novel SRC Kinase Inhibitor TG100435 and its *N*-oxide metabolite by Flavin-containing Monoxygenases and Cytochrome P450 Reductase

Ahmed Kousba, Richard Soll, Shiyin Yee and Michael Martin

TargeGen, Inc. 9380 Judicial Drive, San Diego, CA 92121

DMD Fast Forward. Published on September 19, 2007 as DOI: 10.1124/dmd.107.017384
This article has not been copyedited and formatted. The final version may differ from this version.

a). Running Title: *N*-oxidation and retro-reduction by FMO and P450 reductase

b). Corresponding Author: Ahmed Kousba, MD, Ph.D.

Department of Pharmaceutical Property Assessment, TargeGen, Inc., 9380 Judicial Drive, San Diego, CA 92121

T: 1-858-964-2161

F: 1-858-678-0762

Email: akousba@targegen.com

c). Number of text pages 36

Number of tables 1

Number of Figures 8

Number of references 36

Number of words in the abstract 220

Number of words in the introduction 615

Number of words in the discussion 792

d). Non-standard abbreviations: Cytochrome P450 monooxygenases, CYP; flavin containing monooxygenases, FMO; High performance liquid chromatography, HPLC; Liquid chromatography-triple quadrupole mass spectrometry, LC/MS/MS;

ABSTRACT:

TG100435 is a novel multi-targeted Src family kinase inhibitor with demonstrated anti-cancer activity in preclinical species. Potent kinase inhibition is associated TG100435 and its major *N*-oxide metabolite (TG100855). The objectives of the current study were to identify the hepatic enzyme(s) responsible for (1) the total metabolic flux of TG100435, (2) the formation of TG100855 and (3) the subsequent metabolism of TG100855. Flavin-containing monooxygenases (FMO) and cytochrome P450 monooxygenases (CYP) contribute to TG100435 total metabolic flux. TG100435 metabolic flux was completely inhibited by methimazole and ketoconazole suggesting FMO and only CYP3A4 mediated metabolism. TG100855 formation was markedly inhibited (~90%) by methimazole and heat inactivation (>99%). FMO3 was the primary enzyme responsible for TG100855 formation. In addition, an enzyme mediated retro-reduction of TG100855 back to TG100435 was observed. The *N*-oxidation reaction was approximately 15-times faster than the retro-reduction reaction. Interestingly, the retro-reduction of TG100855 to TG100435 in recombinant CYP or liver microsomes lacked inhibition by the CYP inhibitors. TG100435 formation in the human liver microsomes or recombinant CYP increased as a function of cytochrome P450 reductase activity suggesting potential involvement of cytochrome P450 reductase. The results of this *in vitro* study demonstrate the potential of TG100435 and TG100855 to be interconverted metabolically. FMO seem to be the major *N*-oxidizing enzymes while cytochrome P450 reductase appears to be responsible for the retro-reduction reaction.

TG100435 ([7-(2,6-Dichloro-phenyl)-5-methyl-benzo[1,2,4]triazin-3-yl]-[4-(2-pyrrolidin-1-yl-ethoxy)-phenyl]-amine) is a novel multi-targeted Src kinase inhibitor. Src is the prototype member of the Src-family of tyrosine kinases, which comprises eleven highly homologous proteins including Src, Yes, Fyn, Lyn, Hck, Blk, Brk, Fgr, Frk, Srm and Yrk (Trevino *et al.,* 2006). Src is dysregulated in several types of cancers and is involved in tumor progression and metastases (Summy and Gallick, 2006). Src inhibitors have a potential utility in the treatment of various kinds of cancers. TG100435 is the first benzotriazine Src inhibitor (Noronha *et al.,* 2007). The anti-cancer activity of TG100435 was demonstrated in preclinical species with enzymatic potency residing in itself and its major *N*-oxide metabolite TG100855 ([7-(2,6-Dichloro-phenyl)-5-methyl-benzo[1,2,4]triazin-3-yl]-{4-[2-(1-oxy-pyrrolidin-1-yl)-ethoxy]-phenyl}-amine).

As described by Hu *et al.,* (2007) TG100855 is the major metabolite of TG100435 observed in several preclinical species and in human, dog, rat and mouse liver microsomes. While most oxidation reactions lead to inactive metabolites (Carmella *et al.*, 1997; Krueger *et al.*, 2006; Cashman and Zhang, 2006), active metabolites, such as TG100855, have been demonstrated *in vitro* and *in vivo* (Kireter *et al.,* 1984; Hu *et al.*, 2007).

N-oxidation of tertiary amines is a common metabolic pathway and has been mainly attributed to both cytochrome P450 monooxygenases (CYP) and flavin-containing monooxygenases (FMO) (Overby, *et al.*, 1997; Tugnait, *et al.,* 1997). Few studies attributed the compounds *N*-oxidation to FMO and not CYP. FMO and CYP play an important role in the drug oxidative metabolism. FMO represent the major mammalian non-CYP oxidative enzymes (Rettie, *et al.,* 1995). Many more examples of CYP-

mediated metabolism have been reported compared with FMO. This could be attributed to FMO thermal liability in the absence of NADPH, the paucity of reported data, the relative similarity in the types of metabolites produced by FMO and CYP or possibly the use of inadequate bioanalytical methods (Cashman and Zhang, 2006). However, FMO family has gained increasing attention in the last decade. This may be a consequence of an increased emphasis of drug metabolism in drug development and the recognition that introduction of functional groups such as tertiary amines or sulfides into drug candidates that are metabolized by FMO could help decrease adverse drug-drug interactions (Cashman and Zhang, 2006). Unlike CYP, FMO are not easily induced nor readily inhibited by environmental chemicals or drugs (Cashman and Jhang, 2006). Incorporation of tertiary amine into TG100435 provided a liable site for FMO-mediated metabolism.

In the current study, an oxidation-reduction cycling was observed between TG100435 and TG100855. The biological retro-reduction of several *N*-oxide metabolites has been reported in the literature. For example, clozapine *N*-oxide, tamoxifen *N*-oxide and phenethyl hydroxylamine have been shown to from clozapine, tamoxifen and phenethylamine in human liver microsomes, respectively (Lin and Cashman, 1995; Pirmohamed *et al.,* 1995; Parte and Kupfer, 2005). However, very little is known about the associated enzyme(s) responsible for biological retro-reduction of various *N*-oxide metabolites (Parte and Kupfer, 2005).

Therefore the objectives of the current study were to identify the hepatic enzyme(s) responsible for (1) the total metabolic flux of TG100435, (2) the formation of TG100855 and (3) the subsequent metabolism of TG100855. *In vitro* identification of drug-metabolizing enzymes helps to predict the potential for *in vivo* drug-drug

interactions, the impact of polymorphic enzyme activity on drug disposition and the formation of toxic or active metabolites. Data for the *in vitro* drug metabolism are commonly used in the pharmaceutical industry as one of the main criteria for selecting the compounds which are expected to possess commercially acceptable pharmacokinetic characteristics. The enzymes associated with TG100435 metabolic flux, its *N*-oxidation to TG100855 and the retro-reduction of TG100855 to TG100435 were identified in human liver microsomes and human recombinant CYP and FMO using selective and non-selective enzyme inhibitors and different incubation conditions.

Material and Methods

Test Materials

TG100435, TG100855 and a chemical analog used as an internal standard were synthesized at TargeGen Inc. Ketoconazole, methimazole, 1-aminobenzotriazole, furafylline, sulfaphenazole, tranylcypromine, quinidine, midazolam, hydroxy midazolam, phenacetin, paracetamole, mephenytoin, hydroxy mephenytoin, tolbutamide, hydroxy tolbutamide, dextromethorphan, dextorphan, NADPH and NADPH regeneration system (2% sodium bicarbonate, 1 mM β-Nicotinamide adenine dinucleotide phosphate, 5 mM glucose-6-phosphate, and 1 U/ml glucose-6-phosphate dehydrogenase) were purchased form Sigma Chemical Company (St. Louis, MO). Pooled mixed gender human liver microsomes and human recombinant CYP isoforms CYP1A2, CYP2C9, CYP2D6, CYP2E1, and CYP3A4 were purchased from Invitro Technologies Inc. (Baltimore, MD). FMO1, FMO3 and FMO5 were purchased from Sigma Chemical Company (St. Louis, MO). Recombinant cytochrome P450 reductase and CYP2C19 were purchased from Invitrogen Corp. (Carlsbad, CA).

Experimental Procedures

(A). Identification of the enzyme(s) involved in TG100435 metabolism

1. Incubations of TG100435 in recombinant CYP isoforms

The assay conditions were optimized for the incubation time and protein concentrations. TG100435 was incubated at a final concentration of 1 μM in 100 pmol/ml of human recombinant CYP1A2, CYP2C9, CYP2C19, CYP2D6, CYP2E1, or CYP3A4 baculosomes in potassium phosphate buffer (0.1 M; pH 7.4) in the presence or the absence of NADPH regeneration system. The total incubation volume was 0.5 ml. All

samples were pre-incubated in triplicates at 37°C for 5 min. The reactions were started by the addition of TG100435 and samples were then incubated at 37°C for 0 and 60 min. The control samples for assessing the non-enzymatic metabolism of TG100435: a) TG100435 in potassium phosphate buffer, b) TG100435 in potassium phosphate buffer plus NADPH regeneration system, c) TG100435 in potassium phosphate buffer plus enzyme and d) TG100435 in potassium phosphate plus enzyme where 0.5 ml of 100% ice-cold acetonitrile was added first to terminate the reaction followed by the addition of the NADPH regeneration system. The disappearance of TG100435 following incubation with CYP3A4 was linear for protein concentrations between 50 and 400 pmol/ml and an incubation time of 15 to 120 min.

2. Incubations of TG100435 in human liver microsomes

The metabolic stability of TG100435 was evaluated in pooled mixed gender human liver microsomes. The microsomal activity was confirmed and the experimental conditions were optimized with respect to the incubation time and microsomal protein concentrations. The disappearance of TG100435 was linear for protein concentrations between 0.5 and 2 mg/ml and an incubation time of 10 to 60 min. The human liver microsomes (1 mg/ml) were pre-incubated with NADPH regeneration system at 37°C for 5 min. The reactions were started by the addition of TG100435 at a final concentration of 1 μM and samples were then incubated at 37°C for up to 60 min. TG100435 was also incubated in the presence or the absence of the broad spectrum CYP inhibitor 1-aminobenzotriazole (2 mM), the specific CYP3A4 inhibitor ketoconazole (1 μM) or the FMO competitive inhibitor methimazole (25 μM). The incubation conditions of

methimazole were optimized to avoid its potential inhibitory effects on the CYP (Rawden *et al.*, 2000).

3. Incubation of TG100435 in cryopreserved hepatocytes

The metabolic stability of TG100435 was evaluated in human cryopreserved hepatocytes. The hepatocytes were stored in liquid nitrogen until the time of the experiments. After removal from the liquid nitrogen, the vials were uncapped for few seconds then recapped and put over ice for 5 min. Thawing was achieved by gently shaking the vials of hepatocytes in a 37°C water bath for up to 90 sec. As soon as all contents had been thawed, the vials were placed immediately on ice and suspended in 15 ml thawing buffer followed by centrifugation at 50*g* for 5 min. The supernatant was discarded and the pellet containing the hepatocytes was resuspended in the incubation buffer to a volume of 1 ml. The hepatocytes viability determined by trypan blue exclusion was 70%. The hepatocytes were further diluted in incubation buffer to yield final hepatocytes concentration/incubation of $5x10^5$ cell/ml. TG100435 (1 µM) was incubated in the diluted hepatocytes in a final mixture volume of 500 µl at 37°C and 95% O_2/5% CO_2 for up to 3 h. The control samples included either TG100435 incubation in buffer that did not contain hepatocytes or incubation of buffer that contained hepatocytes where 0.5 ml of 100% ice-cold acetonitrile was added first to terminate the reaction followed by the addition TG100435.

(B). Identification of the enzyme(s) responsible for TG100855 formation

1. TG100855 formation in human liver microsomes

Initial studies confirmed the activity of FMO in the utilized liver microsomes using FMO selective substrate benzydamine (Stormer, *et al.*, 2000; Cashman and Zhang,

2006). The formation of benzydamine-*N*-oxide following benzydamine incubation in human liver microsomes in the presence or the absence of NADPH regeneration system was evaluated.

To determine metabolic enzyme system associated with TG100855 formation, FMO and CYP activities were selectively inhibited following TG100435 incubation in the presence or absence of 1-aminobenzotriazole or methimazole as described above.

The effect of heat sensitivity on TG100855 formation was evaluated using the method described by Ring *et al.,* (1999). Two sets of microsomal incubations were utilized where NADPH regeneration system was added to one set and was omitted from the other set. Both sets of samples were then pre-incubated for 1 min at 55°C then all samples were placed on ice and TG100435 was added to each sample. Those samples without regeneration system were supplemented with the cofactor. All samples were then incubated at 37°C for up to 60 min. TG100855 formation was compared with TG100855 formation in the standard incubations. For the standard incubations, liver microsomes were pre-incubated at 37°C for 5 min in the presence of NADPH regeneration system and then the reactions were initiated by the addition of TG100435 and incubated at 37°C for up to 60 min. The activity of CYP and FMO are preserved following microsomal pre-incubation at high temperature in the presence NAPDH regeneration system while only CYP activity is preserved in the absence NAPDH regeneration system (Kedderis and Rickert, 1985). The formation of TG100855 following TG100435 incubation in pooled human liver microsomes was linear for protein concentrations between 0.5 and 4 mg/ml and an incubation time of 10 to 120 min.

2. TG100855 formation in human recombinant enzymes

To identify the specific FMO isoform(s) involved in TG100855 formation, TG100435 (25 µM final concentration) was incubated in 200 µg/ml human recombinant FMO1, FMO3, or FMO5 baculosomes. The assay conditions were optimized for the incubation time and protein concentrations. The TG100855 formation showed linear increases as a function of FMO1 and FMO3 protein concentrations of 50 to 400 µg/ml and an incubation time of 5 to 60 min. The total incubation volume was 0.5 ml. Samples were pre-incubated at 37°C for 5 min. The reactions were started by the addition of TG100435 and samples were then incubated at 37°C for up to 45 min. The disappearance of TG100435 and the production of TG100855 during incubation were simultaneously evaluated. The non-enzymatic metabolism of TG100435 depletion or TG100855 formation was evaluated using the control sample conditions described above.

The proportional contribution of each individual FMO isoform towards the formation of TG100855 was normalized to the specific isoform content in human liver microsomes using modification of the approach reported by Rodrigues (1999). Briefly, the slope of the log linear regression analysis of TG100855 formation rate in each individual isoform was multiplied by the isoform content to estimate the corresponding isoform Normalized Rate (NR). The Total Normalized Rate (TNR) was calculated from the summation of the NR of all isoforms. The TNR was utilized to estimate the % TNR for each individual isoform by dividing the NR of an isoform by the (TNR*100)**.** A considerable human liver microsomes interindividual variability in the contents of FMO1 and FMO3 (2 to 20-fold) has been reported in the literature (Haining *et al.*, 1997; Overby *et al.,* 1997; Koukouritaki *et al,*. 2002). Koukouritaki *et al* (2002) reported FMO1 and FMO3 contents of 0.1±0.3 and 26.9±8.6 pmol/mg microsomal protein, respectively.

Overby *et al.,* (1997) reported FMO3 content of 5-100 pmol/mg microsomal protein, and an FMO5 content which is 3 to 4-fold less than FMO3.

(C). Identification of the enzyme(s) responsible for TG100855 metabolism into TG100435

1. In human liver microsomes

Initial studies confirmed the appropriate FMO activity in the utilized liver microsomes as described above. The formation of TG100435 in pooled human liver microsomes was linear for protein concentrations between 0.5 and 4 mg/ml and an incubation time of 20-120 min. To determine metabolic enzyme system associated with TG100435 production from TG100855, the effect of heat sensitivity on TG100435 formation was evaluated as described previously using the method of Ring *et al.,* (1999). TG100435 formation was also evaluated in the presence of the FMO inhibitor methimazole at 0.1 and 1 mM. Additional studies evaluated TG100435 formation in the presence of CYP specific probe substrates and CYP specific and non specific inhibitors. TG100855 (2.5 µM) was incubated in human liver microsomes as described above with a selected probe substrate (at respective K_m concentrations) in the presence or the absence of CYP specific inhibitors (Walsky and Obach, 2004). Phenacetin, tolbutamide, mephenytoin, dextromethorphan and midazolam were used as probe substrates for CYP1A2, CYP2C9, CYP2C19, CYP2D6, and CYP3A4 respectively. Furafylline, sulfaphenazole, tranylcypromine, quinidine and ketoconazole were used for the inhibition of CYP1A2, CYP2C9, CYP2C19, CYP2D6, and CYP3A4 respectively. 1-aminobenzotriazole (1 and 10 mM) was also utilized as non-specific CYP inhibitor to assess TG100435 formation following the inhibition of all CYP. All inhibitors were

utilized at incubation concentrations which are sufficient to induce 90% or more inhibition of the respective CYP isoform activity. The CYP activities were estimated from the rate of metabolite production as a function of incubation time in the presence or the absence of the CYP inhibitor. The effects of increasing the reducing potency of NADPH (over 10-fold) in the incubation medium on the rate of TG100855 reduction to TG100435 were evaluated using the procedure described above.

2. In human recombinant CYP and FMO isoforms

To identify the specific isoform(s) involved in TG100435 formation, TG100855 (2.5 µM final concentration) was incubated in 200 µg/ml human recombinant FMO1, FMO3, or FMO5 or in 100 pmol/ml human recombinant CYP1A2, CYP2C9, CYP2C19, CYP2D6, CYP2E1, or CYP3A4. The assay conditions were optimized for the incubation time and protein concentrations. The formation of TG100435 in human recombinant CYP was linear for protein concentrations between 50 and 400 pmol/ml and an incubation time of 20-120 min. Samples were treated as described previously. The control samples for assessing the non-enzymatic and NADPH-independent metabolism of TG100855 were prepared as follows: a) TG100855 in potassium phosphate buffer, b) TG100855 in potassium phosphate buffer plus NADPH regeneration system, c) TG100855 in potassium phosphate buffer plus enzyme and d) TG100855 in potassium phosphate plus enzyme where 0.5 ml of 100% ice-cold acetonitrile was added first to terminate the reaction followed by the addition of the NADPH regeneration system.

TG100855 (2.5 µM) metabolism to TG100435 was also evaluated in human recombinant CYP in the presence of CYP specific probe substrates and CYP specific and non specific inhibitors as described above.

3. In human recombinant cytochrome P450 reductase

To evaluate the potential association of human cytochrome P450 reductase with TG100435 formation, TG100855 (2.5 μM final concentration) was incubated in human liver microsomes or in potassium phosphate buffer (pH 7.4) in the presence of increasing concentrations of human cytochrome P450 reductase (0, 100 and 500 pmol/ml). The assay conditions were optimized for the incubation time and protein concentrations. The total incubation volume was 0.5 ml. The human liver microsomes or the potassium phosphate buffer (pH 7.4) plus human cytochrome P450 reductase and the NADPH were pre-incubated at 37°C for 5 min. The reactions were started by the addition of TG100855 and samples were then incubated at 37°C for up to 45 min. Samples were treated as described previously and the production of TG100435 was evaluated.

The reductase activity in human liver microsomes was determined spectrophotometerically by measuring the rate of cytochrome c reduction at 550 nm. A mixture of NADPH regeneration system, 3.3 mM magnesium chloride and 0.95 mg/ml cytochrome c in 250 mM potassium phosphate (pH 7.4) was preincubated for 5 min at 37° C. The reaction was initiated by the addition of 0.1 mg/ml protein, and the change of absorbance at 550 nm was monitored. An extinction coefficient for reduced cytochrome c at 550 nm of 19.6 mM^{-1} cm^{-1} was used to calculate the reductase activity. In human liver microsomes, the reductase activity is 367±109 noml/min/mg protein. The estimated activity is consistent with the typical value of 150 to 350 noml/min/mg protein (Rodrigues, 1999; Dudka, *et al.,* 2005; Dudka, 2006). The manufacture predetermined activity of reductase in CYP1A2, CYP2C9, CYP2C19, CYP 2D6 and 3 CYPA4 were

2.12, 1.32, 2.1, 0.85 and 1.1 µmol/min/mg, respectively. The recombinant FMO system did not express any measurable reductase activity.

(D). Determination of the kinetic parameters of TG100855 and TG100435 formation

The kinetic parameters (*Km* and V_{max}) of TG100855 and TG100435 formation were determined in human liver microsomes. Preliminary experiments established the linearity of TG100855 and TG100435 metabolite formation with respect to the incubation time (10-60 min) and the microsomal protein concentrations (0.2-2 mg/ml). The microsomes were pre-incubated with the NADPH regeneration system for 5 min at 37^0C. Increasing concentrations of TG100435 or TG100855 (0.1 – 40 µM) were added to initiate the reaction and the incubation was continued for a period of 45 min at 37^0C. The total incubation volume was 0.5 ml. The non-enzymatic formation of TG100855 and TG100435 was evaluated as described above.

All reactions were terminated by the addition of 500 µl of 100% ice-cold acetonitrile to each vial followed by the addition of 20 µl internal standard at a final concentration of 0.1 µM. The samples were vortexed for 1 min and centrifuged at 15000*g* for 15 min at 23°C. The supernatant was analyzed for measuring TG100435 and/or TG100855 concentration using liquid chromatography/mass spectrometry (LC/MS/MS).

Analytical Method

LC/MS/MS Waters Quattro LC (Water Technologies) was used for the analysis of TG100435 and TG100855 as follows: 20 µl of the supernatant was injected by a Leap CTC autosampler onto an Agilent1100 HPLC system. Samples were separated using HPLC column Waters Atlantis T3, 100mm x 2.1, 5 µm particle size, and a mobile phase of solvent A (1% formic acid in water) and solvent B (1% formic in 100% acetonitrile)

at flow rate of 0.3 ml/min using LC gradient going from 40% to 65% solvent B for a total run time of 8 min. Samples for the identification of TG100855 metabolite were analyzed at flow rate of 0.3 ml/min using LC gradient going from 5% to 95% solvent B for a total run time of 35 min using HPLC column Waters SymmetryShield RP18, 150mm x 2.1, 3.5 μm particle size. The LC detector uses a starting wavelength of 200 nm and end wavelength of 600 nm. The MicroMass Quattro LC uses electrospray positive (ES^{+ve}) ionization mode; Total Ion Current (TIC) and Multiple Reaction Monitoring (MRM) modes were utilized. The limit of detection was 5 and 10 ng/mL for TG100435 and TG100855, respectively and the inter- and intra-day coefficients of variation did not exceed 15%.

Data Analysis

1. Estimation of TG100435 predicted hepatic clearance

The %TG100435 remaining was used to calculate the half-life ($t_{1/2}$, min) using a log linear regression analysis according the standard pharmacokinetic equation: $t_{1/2}$ = 0.693/slope. The half-life values were scaled to calculate the predicted clearance according to the equations described by Obach (1999):

In human liver microsomes

(CL_{INT}) =

$$0.693 \times 1/t_{1/2} \times (g\ liver\ \ weight/kg\ bw) \times (ml\ incubation/mg\ microsomal\ protein) \times (45\ mg\ microsomal\ protein/g\ liver\ weight)$$

The human physiological standard value of 21 g/kg for the g liver weights/kg body weight (bw) and a 45 mg microsomes/g liver were used (Obach, 1999).

In human hepatocytes

(CL_{INT}) =

DMD Fast Forward. Published on September 19, 2007 as DOI: 10.1124/dmd.107.017384
This article has not been copyedited and formatted. The final version may differ from this version.

$$0.693 \times 1/t_{1/2} \times (g\ liver\ weight/kg\ bw) \times (ml\ incubation/number\ of\ cells/incubation) \times (number\ of\ cells/g\ liver\ weight)$$

The standard value of the hepatocellularity of $12x10^7$ hepatocytes/gm was used (Bayliss *et al.*, 1999).

2. **Calculation of the kinetic parameters for TG100855 or TG100435 formation**

The apparent *Km* and V_{max} of TG100855 or TG100435 formation were estimated using the one and two site Michaels-Menten models. Each model was fitted to the untransformed data of the rate of metabolite formation vs. the substrate concentration using the nonlinear regression program Prism version 4.01. The transformed data was also analyzed by Line-Weaver Burck plot, 1/S (1/substrate concentration) vs. 1/v (1/rate of metabolite formation).

The statistical analysis of the data was limited to the determination of a mean ± standard deviation (SD) for the samples (n=3) by using the standard equations available in Excel. The values for metabolites formation in the samples were compared with the control values using Student's unpaired t test. The levels of significance were considered at $p \leq 0.05$.

Results

TG100435 metabolism in human recombinant CYP, liver microsomes and hepatocytes. To identify the enzyme responsible for the metabolic flux of TG100435, the study utilized the major human recombinant CYP isoforms involved in the drug metabolism. Incubation of TG100435 for 60 min in 100 pmol/ml of human recombinant CYP1A2, CYP2C9, CYP2C19, CYP2D6, CYP3A4 or CYP2E1 displayed metabolic conversion in only the CYP3A4 samples (33 ±2.5% disappearance of TG100435). There was no observable disappearance of TG100435 following its incubation in CYP1A2, CYP2C9, CYP2C19, CYP2D6 or CYP2E1 or in the control samples.

In the human liver microsomes, the use of the CYP inhibitors ketoconazole and 1-aminobenzotriazole resulted in approximately 50% inhibition of TG100435 total metabolic flux **(Table 1)**. The *in vitro* estimated $t_{1/2}$ values of TG100435 disappearance in human liver microsomes in the presence of ketoconazole or 1-aminobenzotriazole were 290 and 250 min, respectively compared with a $t_{1/2}$ value of 124 min determined in the absence inhibitors (**Table 1**). The corresponding TG100435 predicted intrinsic clearance value decreased from 2.9 ml/min/kg to 1.3 and 1.4 ml/min/kg in the presence of ketoconazole and 1-aminobenzotrizole, respectively (**Table 1**). Non-enzymatic depletion of TG100435 was not observed in controls. Incubation of TG100435 in human hepatocytes yielded a predicted intrinsic clearance value of 3 ml/min/kg which is approximately equal to the predicted value determined in the liver microsomes in the absence of inhibitors **(Table 1)**. Co-incubation of TG100435 with a mixture of methimazole and ketoconazole in human liver microsomes resulted in complete inhibition of TG100435 metabolism **(Table 1).**

TG100855 formation in human liver microsomes and recombinant enzymes. Figure 2 presents the Total Ion Current (TIC) and spectrum chromatogram of TG100435 following *in vitro* metabolism in liver microsomes for 0 and 120 min compared with the chromatogram of the synthetic standards of TG100435 and TG100855. The major metabolite peak appears at a retention time of 20.05 min and m/z of 510.6 **(Figure 2A)**. This peak displayed an HPLC retention time and a mass spectrum identical to the synthesized TG100855 (**Figure 2**). TG100855 was stable under the current experimental conditions and showed no analytical interference with TG100435 **(Figure 2).** The CYP3A4 metabolic products were not observed at detectable levels in the current study. This observation is consistent with previously reported results of Hu, *et al.,* (2007) who reported that TG100855 was the only metabolite observed in the human liver microsomal incubations.

The metabolic enzyme system associated with TG100855 formation was determined following selective inhibition of FMO and CYP activities. The effects of 1-aminobenzotrizole and methimazole on TG100855 formation are presented in **Figure 3A**. Incubation of TG100435 with methimazole or with a mixture of methimazole and 1-aminobenzotriazole resulted in marked inhibition of TG100855 formation (~90%) relative to the standard incubations **(Figure 3A)**. In contrast, incubation of TG100435 with 1-aminobenzotriazole did not result in substantial inhibition of TG100855 formation (18%)**.**

TG100855 formation was markedly inhibited (> 99%) following microsomal pre-incubation for 1 min at 55^0C in the absence of NADPH regeneration system relative to the standard pre-incubation for 5 min at 37^0C in the presence of NADPH regeneration

system **(Figure 3B).** In contrast, there was no inhibition of TG100855 formation (0%) in the samples pre-incubated for 1 min at 55^0C in the presence of NADPH regeneration system compared with the standard pre-incubation **(Figure 3B).** The inhibition of FMO mediated TG100855 formation was associated with a 50% reduction in the total clearance of TG100435.

The profiles of the simultaneous TG100435 depletion and the formation of TG100855 following TG100435 incubation in recombinant FMO1, FMO3 and FMO5 are shown in **Figure 4A-C**. FMO3 demonstrated 2.3 and 18x more TG100855 formation than FMO1 and FMO5, respectively **(Figure 4A-C).** Using the range of the reported values for FMO contents in human liver microsomes, the % TNR of TG100855 formation by FMO1, FMO3 and FMO5 were 3.7±4, 94.4±3.6 and 1±0.1%, respectively **(Figure 4D).** Incubation of TG100435 in high concentrations (up to 400 pmol/ml) of recombinant CYP1A2, CYP2C9, CYP2C19, CYP2D6, CYP2E1 or CYP3A4 did not result in any observable TG100855 formation.

TG100855 metabolism in human liver microsomes and recombinant enzymes.

Figure 6 presents the Total Ion Current (TIC) and spectrum chromatogram of TG100855 *in vitro* metabolism in liver microsomes for 0 and 120 min compared with chromatogram of the synthetic standards of TG100435 and TG100855. The major metabolite peak appears at a retention time of 19.28 min and m/z of 494.6 **(Figure 5A)**. This peak showed an HPLC retention time and a mass spectrum identical to the synthesized TG100435 (**Figure 5**).

The rate of TG100435 formation following TG100855 pre-incubation in the human liver microsomes for 5 min at 37°C or 1 min at 55°C in the presence or the

absence of NAPDH regeneration system is shown in **Figure 6A.** TG100435 formation rates in the samples pre-incubated for 1 min at 55^0C were comparable to the formation rates in the samples pre-incubated for 5 min at 37^0C in the presence or the absence of NADPH regeneration system **(Figure 6A).** Therefore heat inactivation of FMO did not inhibit TG100435 formation implying and that FMO is not associated with TG100435 formation. There was no substantial formation of TG100435 in the control samples. As shown in **Figure 6B**, TG100435 formation following methimazole addition was higher than its formation in the standard incubations and increased as methimazole concentration increases **(Figure 6B).**

To identify the enzyme responsible for TG100435 formation, TG100855 was incubated in the major human recombinant CYP and FMO isoforms involved in the drug metabolism. TG100435 was produced in all utilized CYPs, with highest apparent formation by CYP1A2 and CYP2C19**.** The higher levels of TG100435 formation in CYP1A2 and CYP2C19 may be attributed to the elevated reductase activity in these preparations (~2-fold higher than other isoforms). There was no observable TG100435 formation following TG100855 incubation in FMO1, FMO3 or FMO5.

The effects of the prototypical CYP inhibitors (1-aminobenzotriazole, furafylline, sulfaphenazole, tranylcypromine, quinidine or ketoconazole) on the formation of TG100435 following TG100855 incubation in human liver microsomes or in human recombinant CYP are presented in **Figure 7A-C.** Although the utilized isoform specific inhibitors demonstrated more than 90% inhibition of CYP activity, there was no observable inhibition of TG100435 formation in human liver microsomes or in recombinant isoforms **(Figure 7A-C)**. Interestingly, the formation of TG100435 in the

presence of 1-aminobenzotriazole was approximately 3-4x higher than TG100435 formation in the absence of 1-aminobenzotriazole **(Figure 7C)**. Increasing the 1-aminobenzotriazole concentrations in the microsomal incubation resulted in significant increase in the formation rate of TG100435 **(Figure 7C)** accompanied by increase in TG100855 disappearance. The increased formation rate of TG100435 can be attributed to an accumulation of TG100435 due to inhibition of subsequent CYP mediated metabolism. Increasing NADPH concentrations by 10-fold did not result in any appreciable changes in the formation rate of TG100435 following TG100855 incubation in human liver microsomes (data not shown). The formation TG100435 in human liver microsomes supplemented by cytochrome P450 reductase demonstrated increase as a function of the reductase concentrations **(Figure 7D).** Increasing concentrations of cytochrome P450 reductase in potassium phosphate buffer (pH 7.4) did not result in the formation of TG100435 (data not shown) which may be attributed to the absence of co-factors and reconstituted lipid vesicle system required for reductase activity.

Determination of the kinetic parameters of TG100855 or TG100435 formation in human liver microsomes. TG100855 formation in human liver microsomes increases as a function of the incubated TG100435 concentrations **(Figure 8).** The one site model provided a better fit for TG100855 formation than the two site model. The 95% confidence intervals estimated using the one site model ranged from 85.95 to 223.4 for the V_{max} and from 5.658 to 53.87 for the *Km.* The two site model yielded 95% confidence intervals ranged from 0 to $4.54e^{9}$ for $V_{max}1$ and $V_{max}2$, 0 to $4.19e^{7}$ for *Km*1 and from 0 to $1.205e^{7}$ for *Km*2. The calculated *Km* and V_{max} values of TG100855 formation using the one site model were 30 μM and 154 pmol/min/mg protein, respectively **(Figure 8).** The

corresponding intrinsic clearance value (V_{max} /*Km*) was 5.2 µl/min/mg proteins. Transformation of these data to Line Weaver Burck plot shows no evidence of nonlinearity for the *N*-oxidation reaction **(Figure 8B).** The intrinsic clearance for *N*-oxide formation should theoretically be 50% of the total intrinsic clearance in liver microsomes. The intrinsic clearance value of 5.2 uL/min/mg protein is scales to 4.7 mL/min/kg hepatic intrinsic clearance; which is equivalent to the intrinsic clearance of TG100435. This deviation from theoretical could be the result of the inter-conversion of TG100855 and TG100435.

TG100435 formation in human liver microsomes increases as a function of the incubated TG100855 concentrations **(Figure 8).** The single site model provided a better fit for TG100435 formation than the two site model. The 95% confidence intervals estimated using the single site model ranged from 4.78 to 7.09 for the V_{max} and from 10.07 to 24.81 for the *Km*. The two site model yielded 95% confidence intervals range from 0 to 63.81 for $V_{max}1$, 0 to 1434 for $V_{max}2$ and 0 to 129.7 for *Km*1 0 to 84126 for *Km*2. The calculated *Km* and V_{max} values of TG100435 formation using the one site model were 17 µM and 6 pmol/min/mg protein, respectively **(Figure 8).** The corresponding intrinsic clearance value (V_{max} /*Km*) was 0.34 µl/min/mg proteins. Transformation of these data to Line Weaver Burck plot shows no evidence of nonlinearity for the retro-reduction reaction **(Figure 8C).**

While the observed rate of retro-reduction is 15-times slower than the rate of oxidation, the only observed metabolic product for TG100855 was reduction back to TG100435 **(Figure 5)**. Overall the retro-reduction pathway represents a minor component in the metabolism of TG100435.

Discussion

The current study identified the enzymes responsible for the total metabolic flux of TG100435, the formation of TG100855 and the retro-conversion of TG100855 back to TG100435. In human recombinant enzymes, CYP3A4 appeared to be the only CYP isoform metabolizes TG100435**.** Human liver microsomal study supported this observation where TG100435 CYP-mediated metabolism was completely inhibited following ketoconazole or 1-aminobenzotriazole **(Table 1).** Ketoconazole is usually utilized to assess CYP3A4 participation in xenobiotics and drug metabolism (Newton, 1995; Sai *et al.,* 2000). 1-aminobenzotriazole is utilized to assess the general participation of all CYP in the metabolism (Ortiz de Montellano *et al.,* 1984).

Since CYP-mediated metabolism accounted only for ~50% of TG100435 total metabolism in human liver microsomes (**Table 1**), an additional enzyme(s) that is NADPH-dependent and is not susceptible to the CYP inhibitors may be involved in TG100435 metabolism. The similarity of TG100435 predicted clearance values using the human liver microsomes and the human hepatocytes **(Table 1)** and the absence of TG100435 phase II metabolism imply that TG100435 hepatic clearance may be due to phase I oxidative metabolism. In the liver microsomes CYP and FMO are the only two NADPH dependent enzyme systems responsible for xenobiotic oxidation. The complete inhibition of TG100435 metabolism following the mixture of ketoconazole and methimazole suggests that CYP3A4 and FMO contribute to the total metabolic flux of TG100435 **(Table 1).**

In human liver microsomes, the main metabolite of TG100435 is TG100855 **(Figure 2).** Methimazole resulted in ~90% reduction of TG100855 formation relative to

the standard incubation **(Figure 3A)** suggesting that FMO are involved in the TG100855 formation**.** Methimazole is a selective competitive substrate with high affinity for FMO and is widely used to inhibit FMO activity (Ziegler, 1990; Tugnait *et al.,* 1997). The association of FMO with TG100855 was also demonstrated by microsomal heating in the absence of NAPDH regeneration system. More than 99% inhibition of TG100855 formation was observed (**Figure 3B).** TG100855 formation was preserved (0% inhibition) in the presence of NAPDH regeneration system **(Figure 3B).** Human FMO heating liability is a useful method to differentiate FMO from CYP in microsomal incubations (McManus *et al.,* 1987; Grothusen *et al.,* 1996).

The utilization of human recombinant FMO indicated that the FMO-dependent TG100855 formation is attributed to FMO1 and FMO3 (major isoform), but not FMO5 **(Figure 4A-D).** Five isoforms of FMO (FMO1-5) have been cloned and sequenced in human (Hines *et al.,* 1994; Cashman, 1995). FMO1 is the predominant isoform in the kidney, lung and fetal liver while FMO3 is the predominant isoform in adult liver. FMO1 and FMO3 have been implicated in the metabolism of many drugs (Cashman, 1995). FMO5 apparently does not catalyze the oxidations of the common FMO substrates, has a narrow substrate specificity and its role in drug or chemical metabolism has not been yet established (Overby, *et al.,* 1995; Cashman and Jhang, 2006). While the current work had focused on the human liver FMO-mediated metabolism of TG100435, human renal FMO1 could contribute to TG100435 extra hepatic clearance due to the high levels of renal FMO1 (47±9 poml/mg protein) (Yeung, *et al.,* 2000).

Interestingly, the main metabolic pathway of TG100855 was its back reduction to the parent compound TG100435 **(Figure 5).** Increasing TG100435 formation as a

function of methimazole concentration **(Figure 6B)** may imply that methimazole prevented the subsequent *N*-oxidation of the produced TG100435**.**

As shown in **Figures 3-7,** TG100435 and TG100855 appear to be metabolically inter-converted in cyclic fashion**.** The levels of either compound will be a sum of the oxidation and reduction reactions. It is difficult to know the exact rate of one reaction without knowing the other. Therefore, the current study investigated the rates and the levels of both compounds simultaneously and in the presence and the absence of various enzyme inhibitors.

Taken together, the linear rates of TG100855 or TG100453 formation demonstrated by Line Weaver Burck **(Figure 8B-C)** and better fit of the single site model suggest that a single enzyme system may be involved in the *N*-oxidation or the retro-reduction reaction. FMO3 appears to be the enzyme associated with the *N*-oxidation as reflected from its % TNR value of 94.4±3.6% **(Figure 4D).** Cytochrome P450 reductase appears to be the enzyme associated with the retro-reduction reaction as reflected from increasing TG100435 formation as a function of the supplemented reductase **(Figure 7C)** and increasing TG100435 formation in CYP1A2 and CYP2C19 which contain the highest reductase activity among the recombinant isoforms.

In summary, FMO and CYP demonstrated comparable contribution to the total metabolic flux of TG100435. The *N*-oxidation of TG100435 to TG100855 was only associated with FMO activity. The retro-reduction of TG100855 back to TG100435 was primarily mediated by the cytochrome P450 reductase activity. This is the first body of work demonstrating the explicit involvement of cytochrome P450 reductase activity in the xenobiotic retro-reductive metabolism.

References

Bayliss MK, Bell JA, Jenner WN, Park GR and Wilson K (1999) Utility of hepatocytes to model species differences in the metabolism of loxtidine and to predict pharmacokinetic parameters in rat, dog and man. *Xenobiotica* **29:** 253–268.

Carmella SG, Borukhova A, Akerkar SA and Hecht SS (1997) Analysis of human urine for pyridine-N-oxide metabolites of 4-(methylnitrosamino)-1-(3-pyridyl)-1-butanone, a tobacco-specific lung carcinogen Cancer. *Epidemiol Biomarkers Prev* **6**: 113-120.

Cashman JR (1995) Structural and catalytic properties of the mammalian flavin-containing monooxygenase. *Chem Res Toxicol* **8:** 165–181.

Cashman JR (2005) Some distinctions between flavin-containing and cytochrome P450 monooxygenases. *Biochem Biophys Res Commun* **338:** 599-604.

Cashman JR and Zhang J (2006) Human flavin-containing monooxygenases. *Annu Rev Pharmacol Toxicol* **46**: 65-100.

Dudka J (2006) Decrease in NADPH-cytochrome P450 reductase activity of the human heart, Liver and lungs in the presence of alpha-lipoic acid. *Ann Nutr Metab.* **50(2):**121-125.

Dudka J, Jodynis-Liebert J, Korobowicz E, Burdan F, Korobowicz A, Szumilo J, Tokarska E, Klepacz R and Murias M (2005) Activity of NADPH-Cytochrome P-450 Reductase of the Human Heart, Liver and Lungs in the Presence of (-)-Epigallocatechin Gallate, Quercetin and Resveratrol: An *in vitro* Study. *Basic Clin Pharmacol Toxicol.* **97(2):** 74–79.

Grothusen A, Hardt J, Brautigam L, Lang D and Bocker R (1996) A convenient method to discriminate between cytochrome P450 enzymes and flavin-containing monoxygenases in human liver microsomes. *Arch Toxicol* **71:** 64-71.

Haining RL, Hunter AP, Sadeque AJ, Philpot RM and Rettie AE (1997) Baculovirus-mediated expression and purification of human FMO3: Catalytic, immunochemical, and structural characterization. *Drug Metab Dispos* **25:**790–797.

Hines RN, Cashman JR, Philpot RM, Williams DE and Ziegler DM (1994) The mammalian flavin-containing monooxygenases: Molecular characterization and regulation of expression. *Toxicol Appl Pharmacol* **125:** 1–6.

Hu, SX, Soll, R, Yee, S, Lohse, DL, Kousba, A, Zeng, B, Yu, X, McPherson, A, Renick, J, Cao, J, Tabak, A, Hood, J, Doukas, J, Noronha, G and Martin, M (2007) Metabolism and pharmacokinetics of a novel Src inhibitor TG100435 and its active *N*-oxide metabolite TG100855. *Drug Metab Dispos* **35:**929–936.

Lin J and Cashman J (1997) N-Oxygenation of phenethylamine to the *trans*-Oxime by adult human liver flavin-containing monooxygenase and retroreduction of phenethylamine hydroxylamine by human liver microsomes. *JPET* **282:** 1269–1279,

Kedderis GL and Rickert DE (1985) Loss of rat liver microsomal cytochrome P-450 during methimazole metabolism. Role of flavin-containing monooxygenase. *Drug Metab Dispo.* **13:** 58-61.

Koukouritaki SB, Simpson P, Yeung CK, Rettie AE Hines RN (2002) Human flavin-containing monooxygenases 1 (FMO1) and 3 developmental expression. *Pediatr Res* **51 (2):** 236-243.

Kireter PA, Ziegler, DM, Hill, KE and Burk RF (1984) Increased biliary GSSG efflux from rat liver perfused with thiocarbamamide substrate for the flavin-containing monooxygenases. *Mol Pharmacol* **26:** 122-127.

Krueger SK, Vandyke JE, Williams DE and Hines RN (2006) The role of flavin-containing monooxygenase (FMO) in the metabolism of tamoxifen and other tertiary amines. *Drug Metab Rev* **38**: 139-47.

McManus ME, Stupans I, Burgess W, Koenig JA, de la Hall PM and Birkett DJ (1987) Flavin-containing monooxygenase activity in human liver microsomes. *Drug Metab Dispos* **15:** 256-261.

Newton DJ, Wang RW and Lu AYH (1995) Cytochrome P450 inhibitors: Evaluation of specificities in the *in vitro* metabolism of therapeutic agents by human liver microsomes. *Drug Metab Dispos* **23:** 154-158.

Noronha G, Barrett K, Boccia A, Brodhag T, Cao J, Chow CP, Dneprovskaia E, Doukas J, Fine R, Gong X, Gritzen C, Gu H, Hanna E, Hood JD, Hu S, Kang X, Key J, Klebansky B, Kousba A, Li G, Lohse D, Mak CC, McPherson A, Palank MSS, Pathak VP, Renick J, Shi Feng, Soll R, Splittgerber U, Stoughton S, Tang S, Yee S, Zeng B, Zhao N and Zhu H (2007) Discovery of [7-(2,6-Dichlorophenyl)-5-methyl-benzo[1,2,4]triazin-3-yl]-[4-(2-pyrrolidin-1-yl-ethoxy)phenyl] amine a potent, orally active Src kinase inhibitor with anti-tumor activity in preclinical assays. *Bioorg Med Chem Lett* **17:** 602-608.

Obach R (1999) Prediction of human clearance of twenty-nine drugs from hepatic microsomal intrinsic clearance data: An examination of *in vitro* half-life approach and nonspecific binding to microsomes. *Drug Metab Dispos* **27:** 1350-1359.

Ortiz de Montellano PR, Mathews JM and Langry KC (1984) Autocatalytic inactivation of cytochrome P-450 and chloroperoxidase by l-aminobenzotriazole and other aryne precursors. *Tetrahedron* **40:** 511-519.

Overby LH, Buckpitt AR, Lawton MP, Atta-Asafo-Adjei E, Schulze J and Philpot RM (1995) Characterization of flavin containing monooxygenase 5 (FMO5) cloned from human and guinea pig: evidence that the unique catalytic properties of FMO5 are not confined to the rabbit orthologs. *Arch. Biochem. Biophys* **317:** 275–84.

Overby LH, Carver GC and Philpot RM (1997) Quantitation and kinetic properties of hepatic microsomal and recombinant flavin-containing monooxygenases 3 and 5 from humans. *Chem Biol Interact* **106:** 29–45.

Parte P and Kupfer D (2005) Oxidation of tamoxifen by human flavin containing monooxygenases (FMO1) and FMO3 to tamoxifen-N-oxide and its novel reduction back to tamoxifen by human cytochrome P450 and hemoglobin. *Drug Metab Dispos* **33:** 1446-1452.

Pirmohamed M, Willams D, Madden S, Templeton E and Park K (1995) Metabolism and bioactivation of clozapine by human liver in vitro. *JPET*, **272:** 984-990.

Rawden, HC, Kokwaro GO, Ward SA, Edwards G (2000) Relative contribution of cytochromes P-450 and flavin-containing monoxygenases to the metabolism of albendazole by human liver microsomes. *Br J Clin Pharmacol* **49:** 313-322.

Rettie AE, Meier GP and Sadeque AJM (1995) Prochiral sulfides as in vitro probes for multiple forms of the flavin-containing monooxygenase. *Chem-Biol Interact* **96:** 3-15.

Ring BJ, Wrighton SA, Aldridge SLK, Hansen K, Haehner B and Shipley LA (1999) Flavin-containing monooxygenase-mediated *N*-oxidation of the M1-muscarinic agonist xanomeline. *Drug Metab Dispos* 27**:** 1099-1103.

Rodrigues AD (1999) Integrated Cytochrome P450 Reaction Phenotyping attempting to bridge the gap between cDNA- expressed cytochromes P450 and native human liver microsomes. *Biochem Pharmacol* **57:** 465-480.

Sai Y, Dai R, Yang TJ, Krausz KW, Gonzalez FJ, Gelboin HV and Shou M (2000) Assessment of specificity of eight chemical inhibitors using cDNA-expressed cytochromes P450. *Xenobiotica* **30:** 327-343.

Stormer E, Roots I and Brockmoller J (2000) Benzydamine N-oxygenation as an index reaction reflecting FMO activity in human liver microsomes and impact of FMO3 polymorphisms on enzyme activity. *Br. J. Clin Pharmacol* **50:** 553–61.

Summy JM and Gallick GE (2006) Treatment for advanced tumors: Src Reclaims Center Stage. *Clin Cancer Res* **12:** 1398-1401.

Trevino JG, Summy JM and Gallick GE (2006) Src inhibitors as potential therapeutic agents for human cancers. *Mini Rev Med Chem* **6**: 109-120.

Tugnait M, Hawes EM, Mckay G, Rettie AE, Haining RL and Midha KK (1997) *N*-Oxygenation of clozapine by flavin-containing monooxygenase. *Drug Metab Dispos* **25:** 524-527.

Walsky L and Obach S (2004) Validated assays for human cytochrome P450 activities. *Drug Metab Dispos* **32:** 647–660.

Yeung CK, Lang DH, Thummel KE, and Rettie AE (2000) Immunoquantitation of FMO1 in human liver, kidney and intestine. *Drug Metab Dispos* **28:**1107–1111.

Ziegler DM (1990) Flavin-containing monooxygenases: enzymes adapted for multisubstrate specificity. *Trends Pharmacol Sci* **11:** 321 -324.

Legends for Figures:

Figure 1. Chemical structures and proposed metabolic pathways of TG100435 and its major *N*-oxide metabolite TG100855.

Figure 2. Chromatograms of the Total Ion Current (TIC) **(A)** and spectrum **(B)** of TG100435 and its metabolite TG100855 in microsomal samples incubated for 0 and 120 min compared with TG100435 and TG100855 synthetic standards. TG100435 (20 μM) was incubated in pooled human liver microsomes (1 mg/ml) as described in the Materials and Method section.

Figure 3. **(A)** The effects of methimazole (Meth), 1-aminobenzotriazole (ABT), or mixture of methimazole and 1-aminobenzotriazole on the formation of TG100855 in human liver microsomes. **(B)** The effect of heat treatment of the human liver microsomes at 55^0C for 1 min on the formation of TG100855 in the presence or the absence of NADPH regeneration system. The data are expressed as % TG100855 formation at different incubation conditions as described in the Materials and Methods section. Each bar represents the mean ± SD of 3 samples per time point. *indicates significant difference from the control at $p \leq 0.05$.

Figure 4. Metabolism of TG100435 using individual human recombinant FMO1 **(A),** FMO3 **(B)** and FMO5 **(C)** isoforms. The data are expressed as area ratio of TG100435 disappearance or TG100855 formation as a function of time. Each bar represents the mean ± SD of 3 samples per isoform per time-point. **(D)** FMO1, FMO3 and FMO5 %Total Normalized Rate (TNR) of the estimated TG100855 formation in human liver microsomes.

Figure 5. Chromatograms of the Total Ion Current (TIC) **(A)** and spectrum **(B)** of TG100855 and its reduced metabolite (TG100435) in microsomal samples incubated for 0 and 120 min compared with TG100435 and TG100855 synthetic standards. TG100855 (20 μM) was incubated in pooled human liver microsomes (1 mg/ml) as described in the Materials and Method section.

Figure 6. The rate of TG100435 metabolite formation in human liver microsomes following **(A)** pre-incubation of TG100855 at 37^0C for 5 min and at 55^0C for 1 min in the presence or the absence of NADPH regeneration system (NRS) and **(B)** incubation of TG100855 in the presence of increasing concentrations of methimazole (Meth). The data are expressed as rate (pmol/mg protein) of TG100435 as a function of time. Each data point represents the mean ± SD of 3 samples. *indicates significant difference from the control and ** indicates significant difference from the previous values at $p \leq 0.05$.

Figure 7. Rate of formation of TG100435 (pmol/min) following incubation of TG100855 in the presence or the absence of prototypical CYP inhibitors in human recombinant CYP isoforms **(A)** or human liver microsomes **(B).** Furafylline (Fur), sulfaphenazole (Sulf), tranylcypromine (Tran), quinidine (Quin) and ketoconazole (Keto) were used for the inhibition of CYP1A2, CYP2C9, CYP2C19, CYP2D6, and CYP3A4, respectively **(C)** the rate of formation of TG100435 in human liver microsomes (HLM) as a function of 1-aminobenzotriazole (ABT) concentrations and **(D)** the rate of formation of TG100435 in human liver microsomes as a function of the spiked recombinant cytochrome P450 reductase (CPR) concentrations. Results presented as the mean ± SD of

3 samples. *indicates significant difference from the control and ** indicates significant difference from the previous values at $p \leq 0.05$.

Figure 8. (A) The rate of TG100855 (filled circles) or TG100435 (open circles) metabolite formation (pmol/min/mg) in human liver microsomes as a function of TG100435 or TG100855 substrate concentrations (μM), respectively. Each data point represents the mean ± SD of 3 samples. **(B)** Line-Weaver Burck plot for the *N*-oxidation reaction; 1/S (TG100435 concentration) vs. 1/V (rate TG100855 formation). **(C)** Line-Weaver Burck plot for the retro-reduction reaction; 1/S (TG100855 concentration) vs. 1/V (rate TG100435 formation). The lines represent the data fit for the corresponding metabolite formation.

DMD Fast Forward. Published on September 19, 2007 as DOI: 10.1124/dmd.107.017384
This article has not been copyedited and formatted. The final version may differ from this version.

Table 1. The estimated half life ($t_{1/2}$) and intrinsic clearance (CL) values of TG100435 in pooled human liver microsomes and pooled human cryopreserved hepatocytes in the absence and the presence of 1-aminobenzotriazole, ketoconazole or a mixture of ketoconazole and methimazole.

	Liver microsomes			**Hepatocytes**
	$t_{1/2}$ min	**CL ml/min/kg**	**% TG100435 depletion at 1 hour**	**CL ml/min/kg**
No inhibitor	124	2.9	32.7	3
Ketoconazole	290	1.3	17.4	—
1-aminobenzotrizole	250	1.4	16.4	—
Mixture	ND	ND	0	—

ND; undeterminable

Figure 1

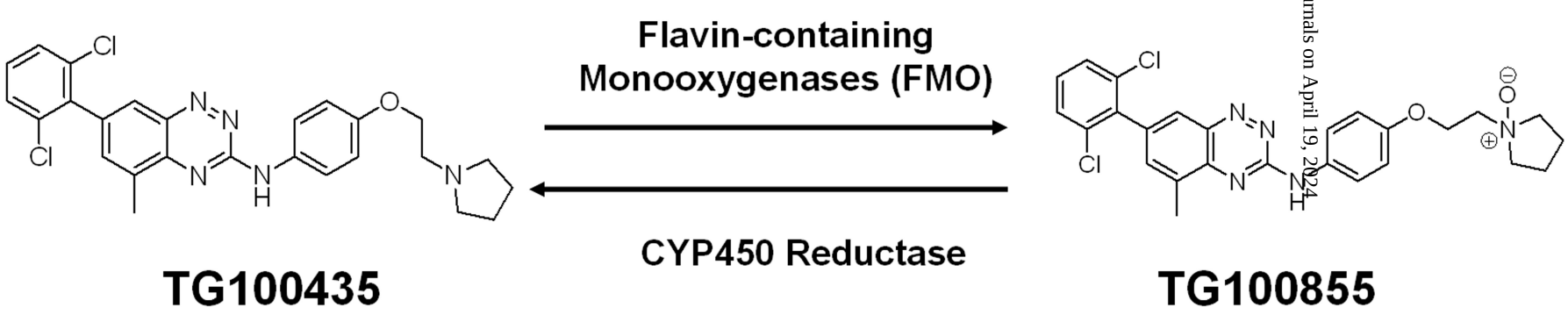

Figure 2

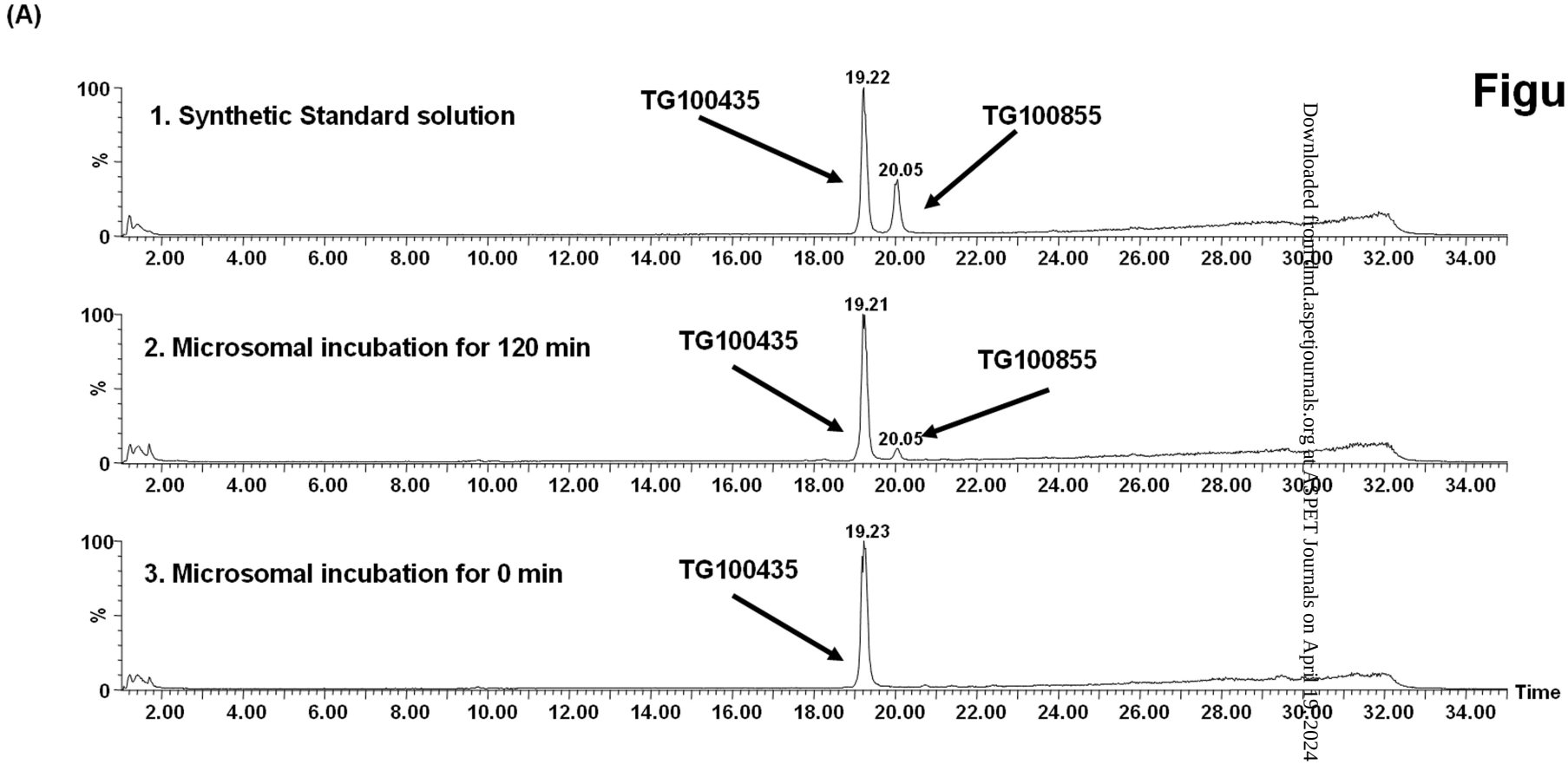

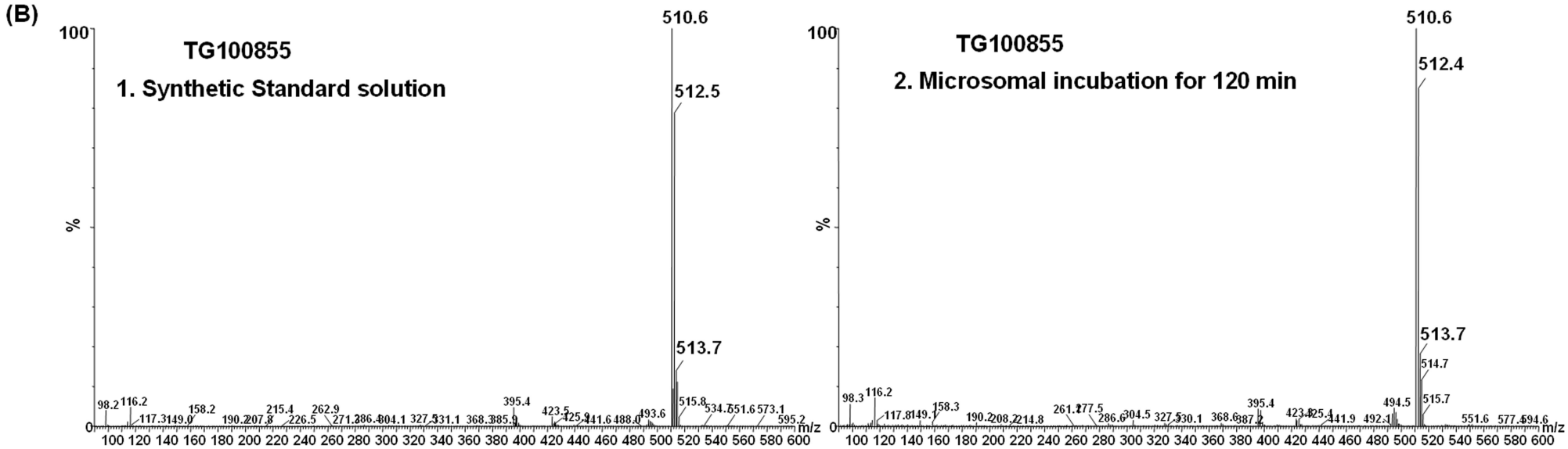

Figure 3

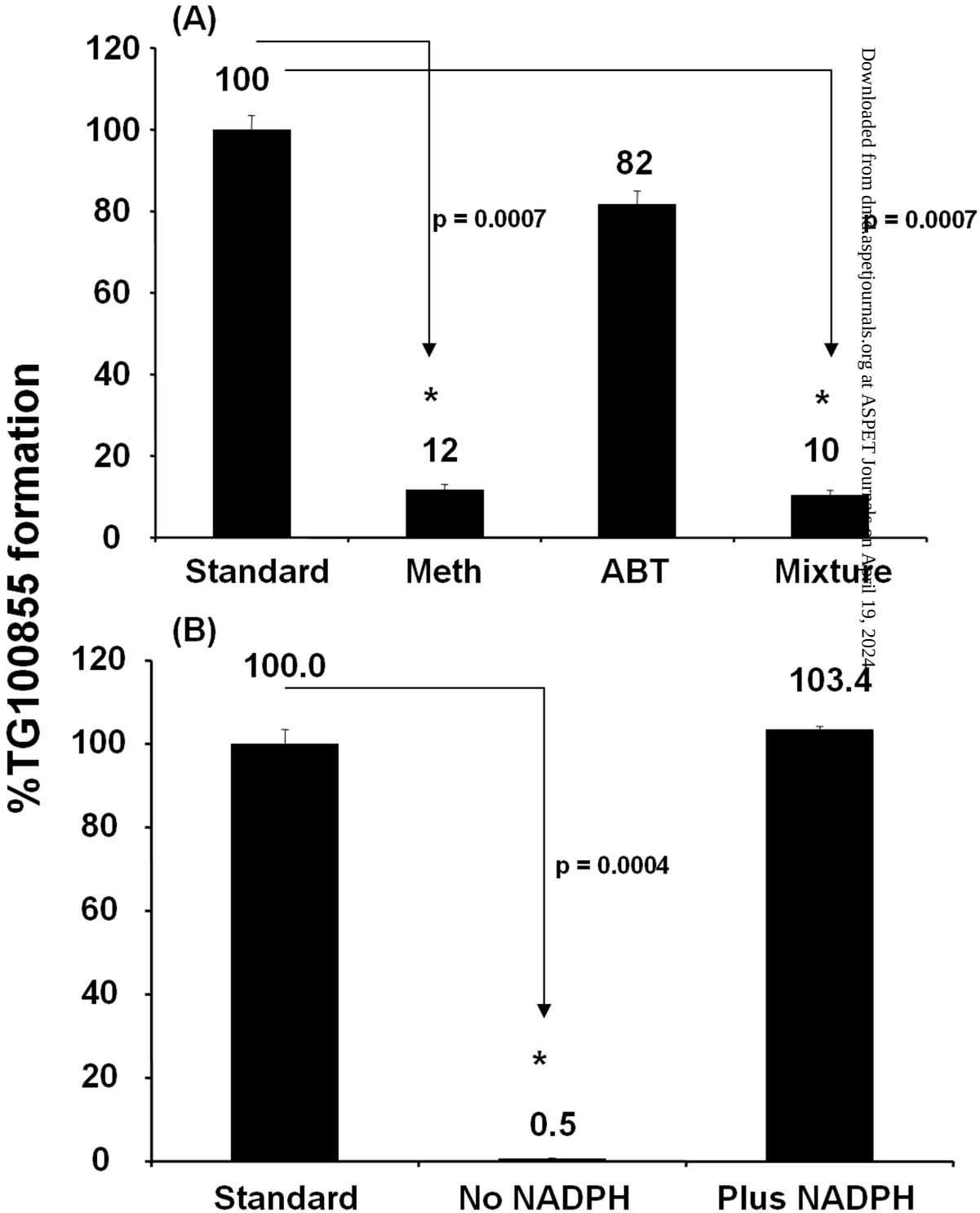

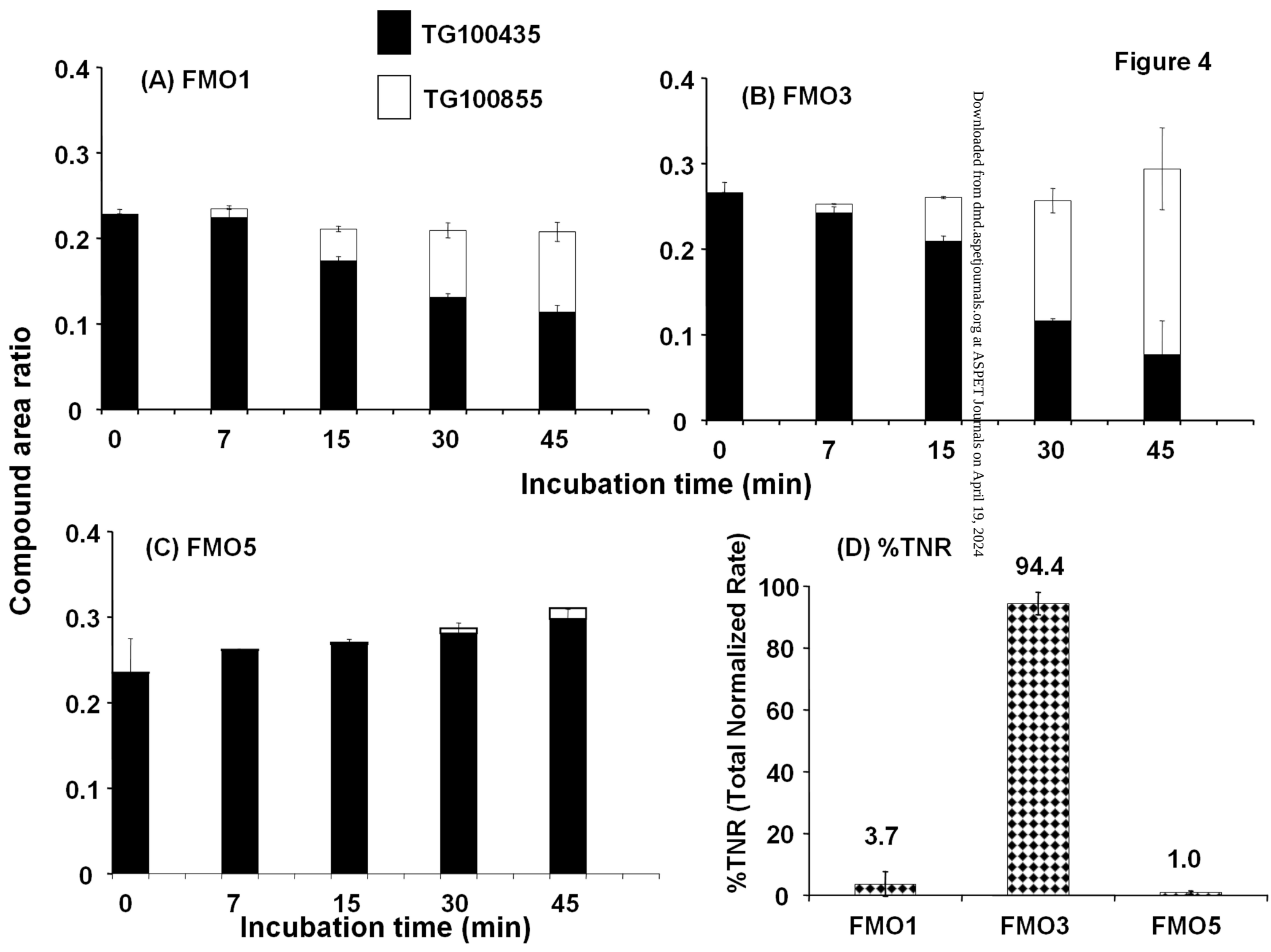

Figure 4

(A)

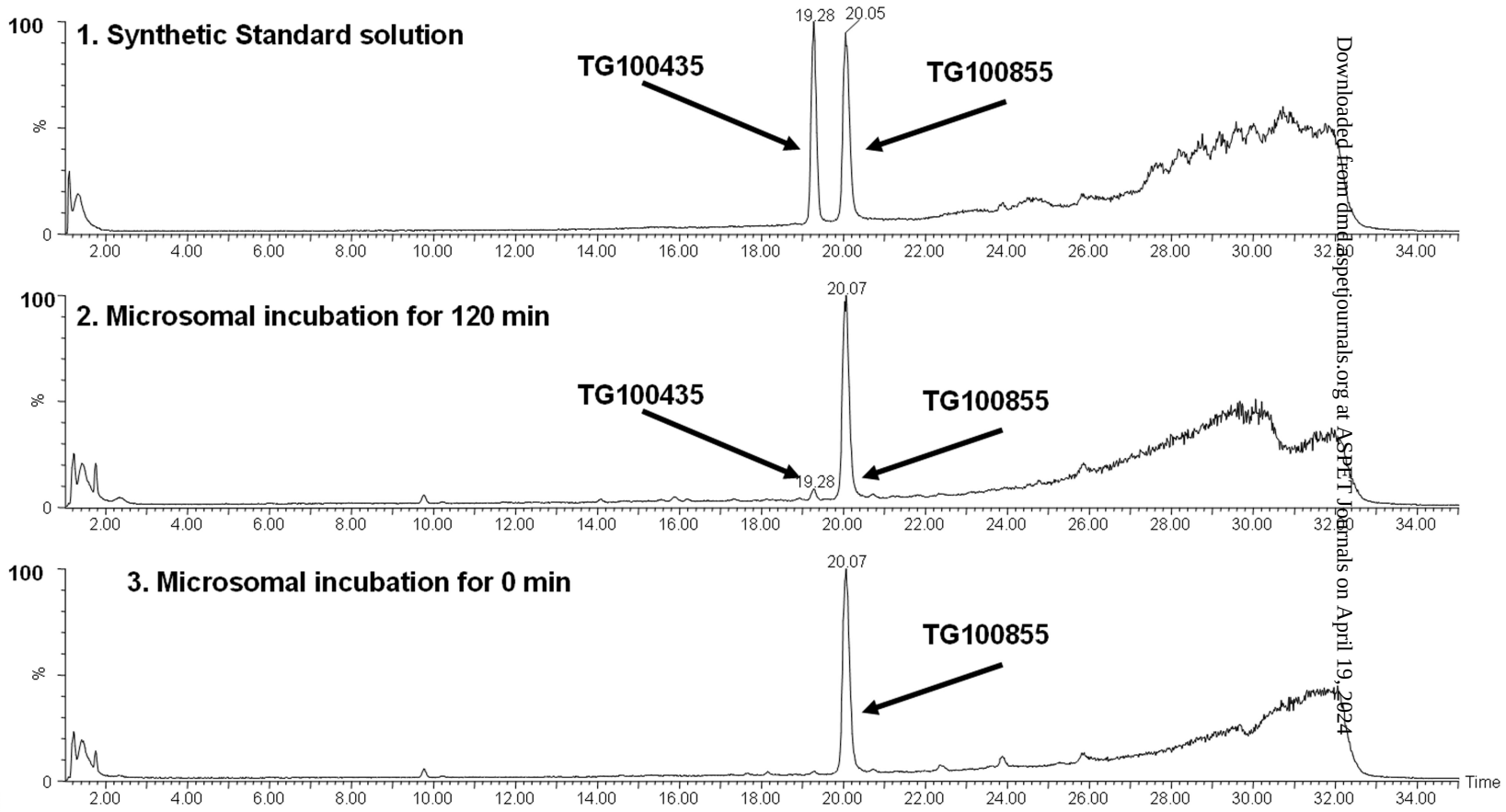

Figure 5

(B)

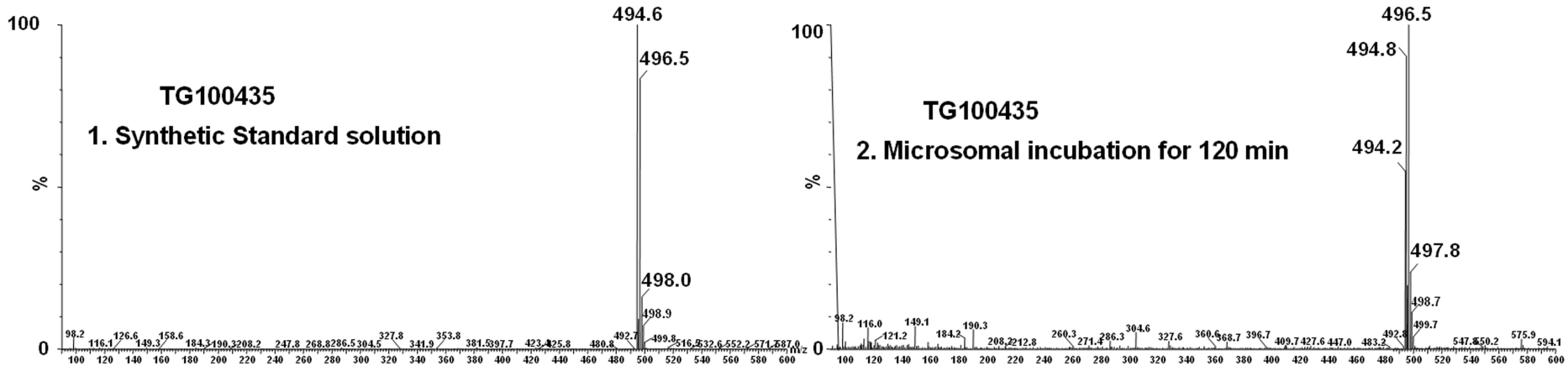

Figure 6

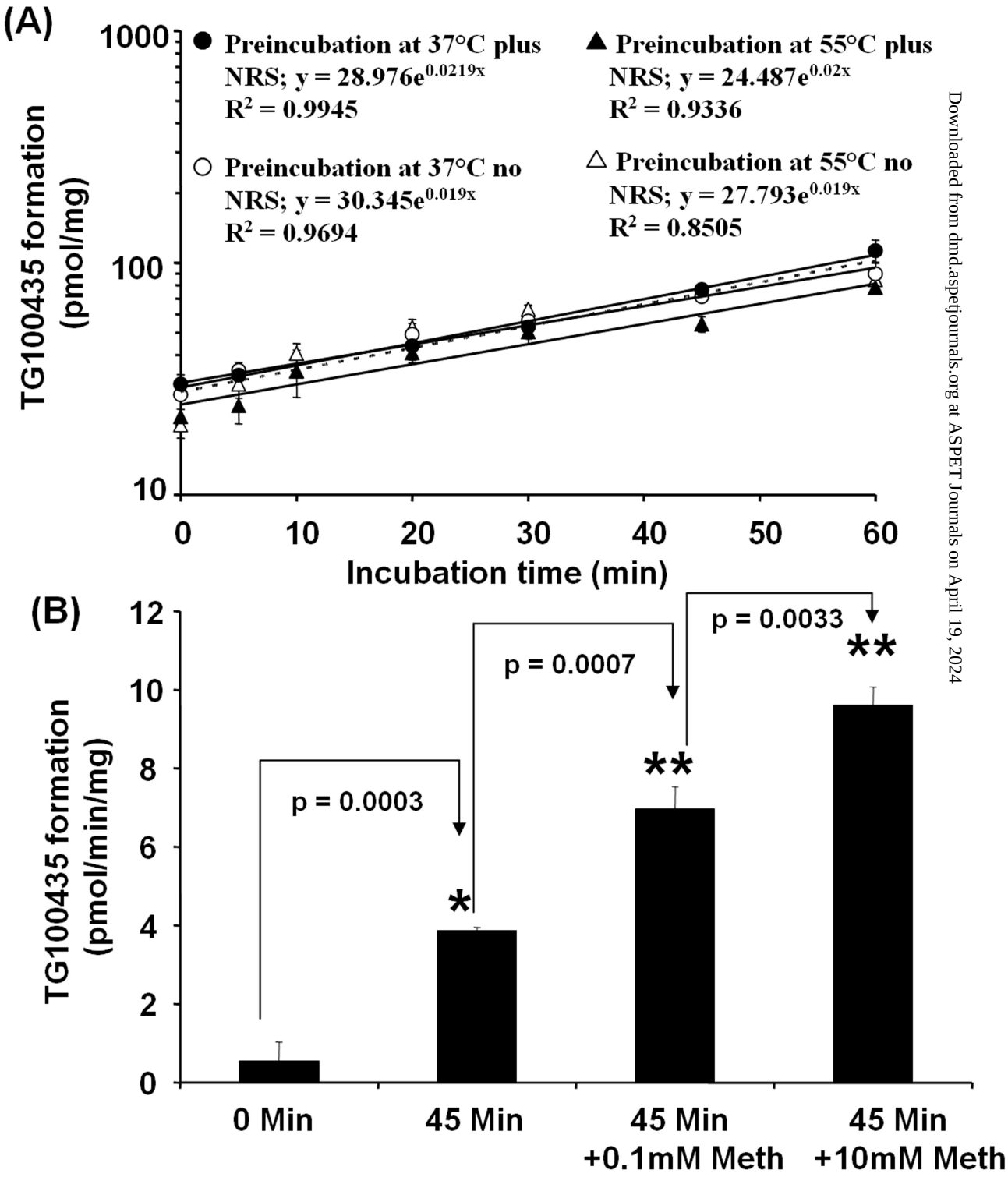

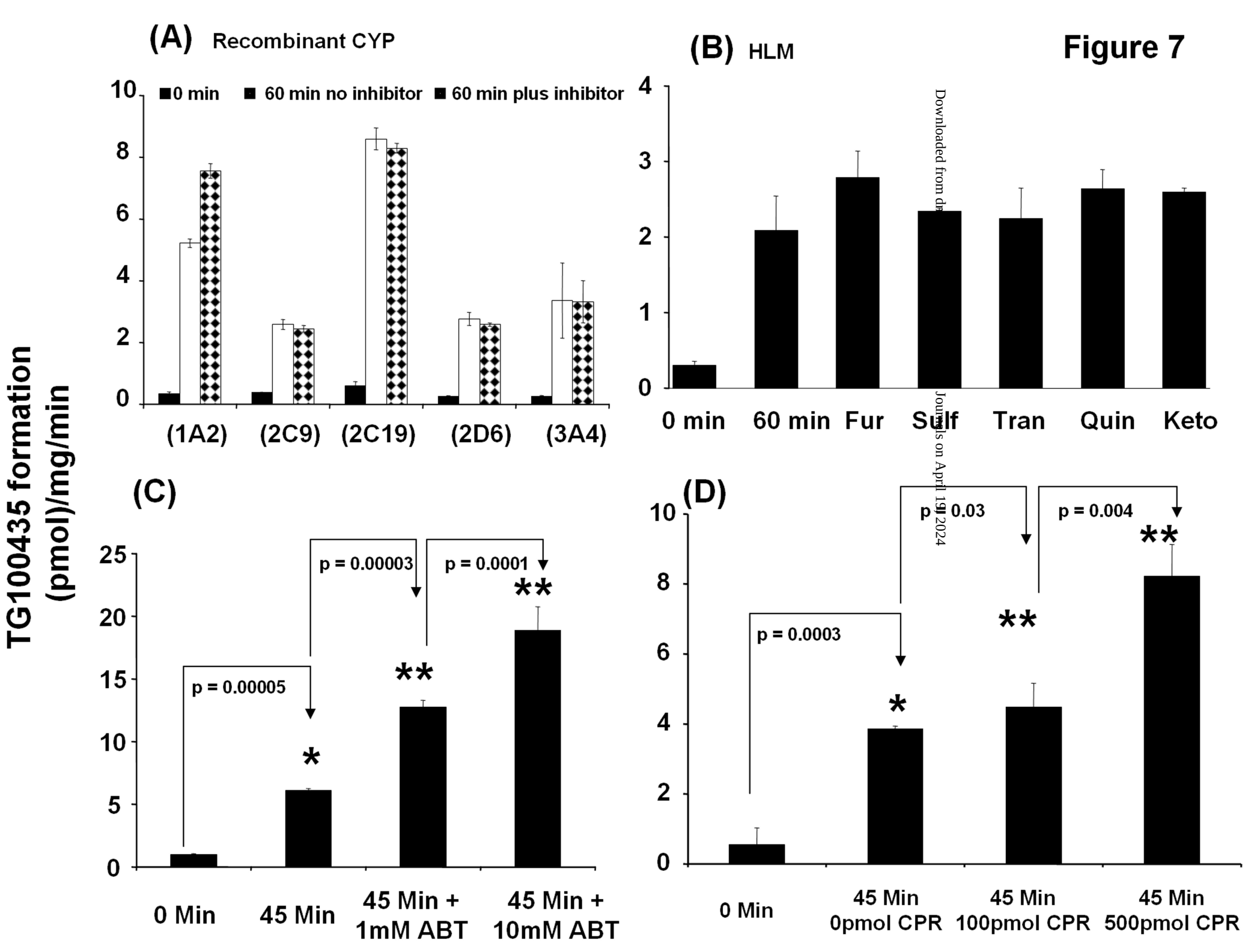

Figure 8